

4101
223

Library T.M.A.L.



TECHNICAL MEMORANDUMS
NATIONAL ADVISORY COMMITTEE FOR AERONAUTICS

No. 683

PROPELLER TIP FLUTTER

By Fritz Liebers

Zeitschrift für Flugtechnik und Motorluftschiffahrt
Vol. 23, No. 9, May 14, 1932
Verlag von R. Oldenbourg, München und Berlin

1.10.4

Washington
September, 1932



3 1176 01437 3527

NATIONAL ADVISORY COMMITTEE FOR AERONAUTICS

TECHNICAL MEMORANDUM NO 683

PROPELLER TIP FLUTTER*

By Fritz Liebers

I. NOTATION

- n, r.p.m.
- λ , frequency in bending.
- λ_0 , frequency in bending of nonrotating propeller
($n = 0$).
- ϵ , length of hub.
- l , free blade length.
- | | | | | |
|----|--------------------|---|--------------|-----------------|
| b, | width of blade | } | b_0, d_0 , | values at root. |
| d, | thickness of blade | | b_l, d_l , | values at tip. |
- α , angle of attack (α_l , at blade tip).
- $\frac{\partial c_a}{\partial \alpha}$, change in air load with angle of attack.

II. INTRODUCTION

As long as wooden propellers were used exclusively in aviation, the problem of propeller tip flutter was practically unknown. But the introduction of the metal propeller, of necessity as thin as possible for reasons of aerodynamics, as well as of weight, has changed these conditions. The number of metal propellers which revealed flutter phenomena when tested on the torque stand, and the number of those damaged or broken in flight because of tip flutter, can no longer be disregarded.

*"Versuche " über Luftschraubenschwingungen." Zeitschrift für Flugtechnik und Motorluftschiffahrt, May 14, 1932, pp. 251-259.

As to contributory causes, mode, and frequencies of this flutter, any set opinion based upon observation is difficult. The eye does not perceive the deformations of the propeller when in motion, nor does the noise, made up of numerous components, admit of acoustic deductions.

Theoretically, one might at first liken these vibrations to those observed on airplane wings, that is, to unstable vibrations. But the mathematical pursuance of this assumption showed this kind of vibrations to be extremely improbable for propellers. The reason lies in the very high torsional stiffness of the propeller blade as compared to the air loads impressed upon it, in the inferior coupling between torsional and bending vibrations of the blade and in the material discrepancy between the torsional and bending frequencies which are in proportion of about 10:1.*

Another explanation is to visualize the tip flutter as being due to the periodic eddy separation from the boundary layer. Estimation for this case - with the little information available - the eddy separation frequencies for a propeller blade of usual speed and size yields figures which are far beyond the natural frequencies of propeller blades at the outer sections, and a resonance between eddy separation frequencies and torsion frequencies of the blade as entirely feasible for sections to about one-half radius. Premises for the vibrations are: ample energy within the eddy separation to assure its periodic sequence under the given conditions. Elucidation of the problem awaits further experiments of eddy separation on profiles with relation to the angle of attack.

Apart from these two there are a number of conditions which may be cited as possible leads to a solution of propeller tip flutter. They need not be enumerated here. The reader is referred to reference 7, in which Seewald treats these problems thoroughly.

The present report is limited to a case of tip flutter recognized by experience as being important. It is the case where outside interferences force vibrations upon the propeller. Such interferences may be set up by the engine, or they may be the result of an unsymmetrical field of flow.

*Compare also the mathematical treatise in reference 6, by Liebers, page 17.

There is only one authentic case where it could be absolutely proved that engine disturbances were the cause of propeller vibrations. That was a resonance between the torsional vibrations of the engine shaft by a critical r.p.m. and the frequency of the first higher harmonics in bending of the propeller at this revolution speed. The particular engine had a torque diagram with unusually high peaks. Ordinarily, however, engine shaft disturbances are not transmitted to the propeller because of the high moment of inertia of the latter. With a view to a future compilation on propeller vibrations, the possibility of higher harmonics in propeller blades excited by the power plant are being studied in detail.

But particular stress is laid upon the seemingly more important second case, that is, excitation of vibration by periodically alternating propeller stresses due to unsymmetry of the field of flow. Because of the low frequency of such interferences, it herein invariably pertains to the first harmonics of the propeller blades.

Adjacent propellers, wings, or other parts of the airplane set up irregularities in velocity and, above all, direction of the air flow. For instance, assume a disturbance in an angle of attack change of the blade by $\Delta\alpha = 1^\circ$, then the loading of the blade, which is, say $\frac{\partial c_a}{\partial \alpha} = 5$, is altered accordingly by

$$\Delta c_a = \frac{\partial c_a}{\partial \alpha} \Delta\alpha = 5 \frac{1}{57.3} = 0.087$$

That means, by an ordinary load of, say, $c_a = 0.6$, a disturbing force of 15 per cent of the normal air load. Such disturbances recur with the revolution, quite frequently even with twice the revolution speed. In the unfavorable case, resonance occurs at which the deflections of the blades may become large.

More than once it has been possible to explain a damaged propeller in this manner. On the other hand, none of the many propellers, whose mathematically defined critical r.p.m. for resonance vibrations was above the maximum r.p.m. of the respective propeller, has at any time shown signs of vibration. This holds true, for instance, for practically all wooden propellers. Furthermore, in several cases where the calculation indicated vibrations in resonance, a torque stand test actually revealed vibrations at the particular r.p.m.

At the same time it was noted that a changed blade setting enlarged the range of resonance - yes, that occasionally vibrations by the anticipated resonance r.p.m. did not set in at all until a certain high blade setting had been reached. A plausible explanation for this occurrence is that at high pitch a decisive part of the sections is appreciably "stalled," as soon as the propeller dips into a zone of interference. Then the respective profiles would not only experience outside disturbances with the period of their natural vibration, in case of resonance, but would at the same time and with the same period reach amplitudes where the additional air loads released by the vibrations no longer damp but (because $\frac{\partial c_a}{\partial \alpha} < 0$) rather intensify the vibrations. Thus the propeller itself draws energy from the air in the same rhythm as the propeller is stimulated to vibration. This may also explain why many propellers run smoothly in flight, even though the torque tests revealed vibrations. (This is merely a conjecture.)

Lastly it might be mentioned that with flexible propellers, whose critical resonance r.p.m. was far below the maximum r.p.m., it was sometimes possible to eliminate the resonance range by increasing the r.p.m., so that the propeller ran smoothly in the super-critical range.

These statements are based on a mathematical analysis of the natural frequencies of propeller blades with respect to the r.p.m.

III. THEORETICAL RESULTS

The results concerning the natural frequencies of propeller blades, based upon the computations outlined in references 5 and 6 are briefly summarized as follows:

First, it is seen that a propeller blade in its two principal degrees of freedom, designated as bending and torsion, has two totally different frequencies in the proportion of about as 1:10. Consequently it is legitimate to disregard the coupling between the degrees of freedom and treat each separately. The basic frequencies of the torsional vibrations* are of the order of magnitude of 10,000 min.⁻¹. They are practically unaffected by the air

*The frequencies are given in min.⁻¹ because they relate to the number of revolutions and this could best be expressed per minute.

loads acting on the propeller and are, in addition, independent, in first approximation, of the centrifugal forces acting on the blade. As to the vibrations forced by outside stimulants, it may be deduced from the height of the torsional vibration figure that in this case the vibrations are scarcely dangerous, because, apart perhaps from the tandem arrangement of two multi-blade propellers, it is difficult to conceive that 10 or more disturbances for each r.p.m. necessary for the resonance case actually do occur with the customary propeller installations.

The fundamental frequencies of the bending vibrations are of the order of magnitude of $1,000 \text{ min.}^{-1}$. Here the air loads are of even less significance than for the torsional vibrations. But the centrifugal forces exert a marked influence on the bending frequency, so that a rotating propeller may attain to twice the vibration figure of the non-rotating propeller. As a result the frequencies within ambit of the service range of the blades may be of the order of magnitude of a small multiple of the number of revolutions. And since unsymmetrical loadings are readily possible at this mode, the propeller can indeed be forced to bending vibrations in resonance.

The conditions for the two degrees of freedom of a propeller blade are now such as to direct our interest especially to a study of the bending vibrations.

1. Determination of Frequencies in Bending

The analysis of the bending vibrations was based upon the well-known Rayleigh principle* of minimum natural frequency of an elastic system. The bending frequency was expressed in the form of **

$$\left(\frac{\lambda}{\lambda_0}\right)^2 = X_1 + X_2 \left(\frac{n}{\lambda_0}\right)^2 \quad (1)$$

where λ = frequency at any revolution n , λ_0 = static frequency ($n = 0$), and X_1 and X_2 = functions containing the dependence of the frequency on the blade shape and of

*Theory of Sound, Vol. I, sections 88 and 89.

**As to the actual calculation method the reader is referred to references 5 and 6.

vibration curve variable with the revolution. (Reference 6, p. 145.) Resolution of equation (1) for differently shaped blades then reveals the significant fact that two propellers - even if different, within large limits, in dimensions, material constants or shape (taper), - but of equal static frequency (λ_0) and equal ratio of hub length to blade length (ϵ/l), have almost concordant bending frequencies when in rotation also.

This is an important result from the practical point of view: it permits of substituting the numerous parameters such as specific weight, elasticity modulus, cross section shape, moment of inertia of section, free blade and hub length by two parameters, namely static natural frequency (λ_0) and ratio of hub length to blade length (ϵ/l). The result is a single formula applicable to propellers of any dimensions or shape:

$$\frac{\lambda}{\lambda_0} = \left[1 + \frac{7 \left(\frac{n}{\lambda_0} \right)^2}{6 + 7 \left(\frac{n}{\lambda_0} \right)} \right] \sqrt{\frac{1 + (1 + 2 \frac{\epsilon}{l}) \left(\frac{n}{\lambda_0} \right)^2}{1 + \left(\frac{n}{\lambda_0} \right)^2}} \quad (2)$$

This equation is an approximation formula arrived at by interpolation of (1) for all possible blade forms. Figure 1 shows ϵ/l for different values. Specific examples for (2) are given in Figures 5 to 8 and 15.

Henceforth the bending frequencies can be readily computed according to equation (2) or Figure 1. One simple deflection test to define static frequency λ_0 is all that is necessary, the rest can be taken from Figure 1.

From the nature of Rayleigh's minimum principle, equation (1) or (2) can yield no other than too high frequency figures. But it is possible to effect a correction, because the frequencies, on the other hand, cannot be lower than dictated by

$$\lambda^2 \geq \lambda_0^2 + (1 + 2 \frac{\epsilon}{l}) n^2 \quad (3)$$

Inequation (3) is derivable direct from (1). (Reference 5.) It is a special case of the general law, first proved by Lamb and Southwell,* according to which, in an elastic system acted upon by several independent forces, the square of the basic frequency is always higher than the sum of the squared frequencies that the system would

*Proc. Roy. Soc. Vol. 99, London, 1921.

have if only one of the forces were active. (A new proof is quoted in reference 6, p. 147.) With only the elastic forces in effect, the frequency of the propeller is λ_0 ; with only the centrifugal forces in action the propeller behaves like a heavy string. Its frequency, up to quantities of higher order,* follows the second summand in (3).

For $n = 0$ and $n = \infty$, equations (2) and (3) merge. In the interim stage the discrepancy, i.e., the greatest error imaginable is less than 7 per cent. (See fig. 10 in reference 6.) Because of the only formal significance of the inferior limit (3) equation (2) is preferable. The actual error with (2) is accordingly much lower than 7 per cent.

2. Influence of Curvature and Edge Condition

Identification of a slight error in (2) however, merely purports that in the role of approximate solution, (2) deviates but little from the exact solution arrived at under the same premises.

One of the lemmas is: the blade is a straight bar, whereas in reality, it is curved and twisted. Its bending is always coupled with torsion and spatial displacements of the outer sections. To disregard these degrees of freedom, on the other hand, signifies a stiffness of the blade and, consequently, an overestimated frequency in bending. So for this reason, equation (2) will necessarily lead to excessive values. At the same time, inequation (3) is obviously applicable to the lowest possible frequencies for the cambered as for the straight blade. Simply insert the correct figure of the static frequency λ_0 , as say, defined by test, and note that the curved blade, its strength removed and considered as being solely under the effect of the centrifugal force, stretches like a heavy string. Its length l increases and limit (3) accordingly shifts slightly downward. By the minor deviations of the bar axis from the straight line in practice, the change in l and in (3) is trifling. Consequently, formula (2) represents a satisfactory approximation for cambered and twisted blades also.

*The vibration formula of the rotating cable fastened at finite distance from the axis of rotation (on a hub) is solvable by Bessel's functions. It is seen that the expression in (3) represents an excellent approximation for the basic frequency. For $\epsilon/l = 0$, λ is exactly = n .

A second simplifying premise is that the position of equilibrium of the blade lies in the plane of rotation while the blade, because of the inherently existing and through the shear load increased finite deflection swings about a position of equilibrium sloping against the plane of rotation. Under the much exaggerated assumption that all sections of the blade were at 10 degrees to the plane sloping toward the plane of rotation,* the frequency of the bending vibrations would scarcely be less than 1.4 per cent.

Another salient feature, from the practical standpoint, is the influence of the edge condition. It was assumed that the blade was rigidly restrained at the root. This condition need not be met in complete measure. It is, for instance, not fulfilled in a wooden propeller where there is no reason to even speak of a restraint at the hub. Now, however, and this holds for wooden as for metal propellers, the course of the inertia moment of the section over the radius is such that the moments of inertia of the root sections compared to those of the actual blade are so great as to be considered as infinite. Then the drop from high to low moments of inertia is very rapid. Defining the point of the sudden change in moment as the hub end, obviously voids the compliance of the condition for rigid blade restraint. But the removal of the constrained condition can only be followed by a decrease in vibration frequencies. But they also cannot become lower than the blade cut off at the defined point and treated as an oscillating heavy string. Thus the inferior limit (3) retains its validity and our frequency formula is applicable to this case also, again under the assumption that the correct static frequency value is substituted for λ_0 .

In summing up, it may be stated that the conditions are very propitious as far as bending vibrations of propellers are concerned. One single formula is applicable to all blade shapes and vibration conditions, provided the static frequency is known.

3. Comparison with other Experiments

The established investigations which in any way treat

*It denoted a blade deflection of 1/5 of its length.

the problem of bending vibration of rotating bars, (references 1 to 4) all arrive at the same result.

$$\lambda^2 = C_1 \lambda_0^2 + C_2 n^2 \quad (4)$$

where C_1 and C_2 are constants. This formula represents a more or less practical approximation depending on how C_1 and C_2 were defined. For instance, the formula given in Hütte Vol. I (reference 2), reads with our symbols as:

$$\lambda^2 = \lambda_0^2 + n^2 \left(0.75 + 1.5 \frac{\epsilon}{l} \right)$$

Compared to (3)*, this formula is everywhere below the lowest limit for the frequencies.

In an earlier report by Southwell and Gough (reference 3), the frequency formula has again the form of (4) with $C_1 = 1$, but has accounted for the possible error by setting up

$$\lambda^2 > \lambda_0^2 + n^2$$

- into which the lower limit (3) passes at $\epsilon/l = 0$. The method disregards the variability of the elastic line with the revolution and overlooks the fact that the blade, owing to attachment at root, is impressed by centrifugal forces other than those of a rod rotating about its end. The omissions are partly neutralized; but the final results still show a marked discrepancy from actuality. (See bottom of fig. 9.) On top of it all, the determination of constant C_2 in (4) by Southwell and Gough necessitates the definition of the elastic line of the static blade for each case, i.e., the previous measurement of the course of cross section and moment of inertia in conjunction with a number of protracted integrations. In contrast to that, the superiority of the handy formula (2) given here is especially noteworthy. It is readily seen that it was profitable to derive the frequency formula (1) with respect to the variability of the elastic line. It revealed the similarity of blades of different shapes under centrifugal forces, and incidentally, led to the interpolation formula (2).

* Where, to conform to the stipulations in Hütte (bar of constant cross section) $1.5 \frac{\epsilon}{l}$ is substituted for $2 \frac{\epsilon}{l}$.

IV. EXPERIMENTS

From the practical point of view, it is desirable to know the actual discrepancies between frequency formula (2) and the actual figures in relation to the above proved maximum possible error. To this end, a number of model tests were carried out.

Observance of similarity between model and full scale could be disregarded, when the typical characteristics of a real propeller, primarily its departures from the straight bar shape, were exaggerated in the model. Accordingly, we used very elementary but strongly curved and twisted metal blades instead of true model propellers, especially since it would have been difficult to make such models flexible enough for an easy evaluation. The influence of all peculiarities in blade shape had to be very clear in spite of the simplification.

In addition, the experiments were so arranged that elastic, centrifugal, and aerodynamic forces assumed the mutual relative magnitude as with real propellers (i.e., about 1:2:0.01) as well as for other similar conditions, so that an error in the assumptions for one of the forces would be conspicuously displayed. This applies primarily to the air loads which were introduced on the basis of static wind-tunnel measurements and defined as negligibly small for the magnitude of the frequency.

1. Experimental Method

The method, originally suggested by F. Seewald, has been described in various publications (reference 7, page 373, also reference 8.)

Briefly outlined (see fig. 2), it consists of a right-sided prism P, rotating about an axis coinciding in the extension of the propeller shaft. The prism, whose base yields the total reflection of the rays (doubling of angles by the reflection) produces a steady picture of the blade tip when rotating with half propeller speed. This principle is applied in the rotoscope,* manufactured by

*S. Pritschow: Optical Device for Observing Rotating Parts in Apparent Rest. V.D.I., 1925, p. 700.

Voigtlander and Son, Braunschweig. Of course, it had to be modified for this particular purpose. Synchronization between propeller and rotoscope is obtained by generator G fitted on the propeller shaft and synchronous motor M (geared 2:1) which drives the prism. But with this set-up the vibratory motions fall perpendicular to the plane of the propeller disk in the direction of vision and are thus scarcely perceptible. As a result, we fitted mirror S on the propeller hub. Now the picture of the blade tip in the rotoscope is such as an observer would see while sitting on the hub and rotating with the propeller and looking along the blade. (Fig. 3.) When the propeller vibrates the picture of the blade tip becomes blurred. To dissolve this impression into discreet vibration pictures, we mounted a high-speed motion picture camera Z behind the rotoscope.

This method is superior to the various stroboscopic methods, for it eliminates only the rotation of the propeller while otherwise producing a perfectly uninterrupted picture. Its objectional feature is the very scrupulous adjustment of the rotoscope axis in the direction of the propeller axis.

In the first experiments with propeller of 2-inch diameter, we encountered great difficulties in obtaining the requisite quantity of light for satisfactory photographs with the high-speed camera. Besides, the vibration amplitudes remained so low as to make the interpretation of the pictures appear too uncertain. On account of that we made steel and duralumin models of from 50 to 80 cm diameter, driven from a small three-phase motor (80 watt, at 1,500 r.p.m.). They were so flexible that deflections of several centimeters were readily excited.

The excitation was achieved by short air blasts from a compressed air tank. As the disturbance increased the blades could vibrate freely. The exposures ranged from 80 to 120 per second, or on an average of from 10 to 15 test points for one full vibration. The time mark on the film was obtained by photographing the stationary background. This appears on the photographs through the rotoscope as one turn through 360° per propeller revolution. Consequently, given the propeller speed, an absolute time record for each picture is obtained.

The developed films were projected on a large opaque disk where they could be readily elaborated. The obtained vibration curves then yield the frequencies with sufficient accuracy. Every test was repeated at least once, yielding discrepancies of from 0 to 3 per cent.

2. Test Results

Model 1. - Straight, nontwisted blade, constant cross section, flat profile. Dimensions: $c = 4.8$ cm, $l = 20.8$ cm, ($c/l = 0.23$), $b = 1.6$ cm, $d = 0.02$ cm.

We started with this simple case because even here the influence of different root sizes and different air loads could be satisfactorily studied. The choice of constant section made comparison with other formulas (see III, 3) very expedient.

Figure 4 is a section of the film photographed at revolution $n = 496$ min.⁻¹. The vibrations of the blade tip can be seen in the different positions of the white strip. The background rotates from picture to picture and gives the time record. (See the white dot on the films.) The film record (fig. 4) is analyzed in Figure 5. Figures 6 to 8 give the corresponding vibration curves for several other revolution speeds.

Model 1 was examined at $n = 0$ to $n = 500$ min.⁻¹, and at pitch $\alpha = 0, 10^\circ$ and 25° . The total results (bending frequencies plotted against revolution speed) are compiled in Figure 9 and compared with the theoretical values conformable to equation (2). It is remarked here, that for the extreme case of constant section, which never occurs in propellers, formula (2) must be written exactly $\frac{3}{2} \frac{c}{l}$ instead of $2 \frac{c}{l}$. The difference amounts to only about 2 per cent, but since it is a matter of comparison, it was taken into consideration.

Calculation and measurement are in satisfactory accord, according to Figure 9, and in a speed range considerably above the $\frac{n}{\lambda_0}$ values of large propellers. The angle of pitch, that is, the magnitude of the load and

consequently the equilibrium position has no appreciable effect on the frequencies of the blade. At 0° , 10° , and 25° pitch the $\frac{\partial c_a}{\partial \alpha}$ values are positive, zero, and negative, respectively. There was no sign of any influence of air loads following $\frac{\partial c_a}{\partial \alpha}$ by those released by the vibrations. Besides, as estimated according to the process (reference 6, page 143) at high speed, say $n = 500^{-1}$, the air loads on the model are about three times as high as for real propellers with respect to elastic and centrifugal forces. Thus, if there had been any tangible influence of the air loads on the vibrations, these experiments would have revealed it.

On the other hand, the air loads make themselves felt very distinctly in some other fashion. They exert a damping effect on the flexural vibrations at normal angles ($\frac{\partial c_a}{\partial \alpha} > 0$). This is clearly seen in Figure 7. At settings approaching maximum lift ($\frac{\partial c_a}{\partial \alpha} = 0$) the influence of the air loads is small (see figs. 5 and 6) for $\alpha = 10^\circ$. At higher angles ($\frac{\partial c_a}{\partial \alpha} < 0$) the air loads act in a forcing sense. Even the primitive formula (11) in reference 6, page 143, reveals, after the material damping is inserted, that $\frac{\partial c_a}{\partial \alpha} < 0$ can lead to a speed at which unstable (forced) flexural vibrations set in. Our experiments revealed the same results, (fig. 8 for $\alpha = 25^\circ$). There are steady vibrations which do not die out. The second portion, in particular, shows how - without perceptible disturbance - the vibrations attain to finite amplitude which is then maintained. Whether or not forced vibrations of the described type have any practical significance for propellers, awaits further investigation, but the greater probability is that they have not.

Figure 9 shows the recorded frequencies and those computed by (2), in conjunction with those conformable to R. & M. No. 766 (reference 3) and those according to Hutte. The main reason of the discrepancy by the English formula is to be found in the omission of the hub effect. Hence the disparity will be still greater (compare Model 2) as the hub is larger (greater c/l). The Hutte formula takes the hub into account, but contains a fundamental error.

Following this discussion of the tests on Model 1, we shall only give the final results for the other models.

Model 2.- Same as Model 1, but larger hub. $\epsilon = 17.6$ cm ($\epsilon/l = 0.85$).

To bring out the influence of hub size on the increased flexural frequencies an exaggerated ratio of $\epsilon/l = 0.85$ was chosen. The results are appended in Figure 9; they also agree well with the theoretical curve from equation (2), thus proving that (2) is also applicable to vibrations in turbine blades.

Model 3.- Straight, non-twisted blade, knife-edged wedge, (linear taper in section, taper of moment of inertia with third power of the radius), plane profile. Dimensions: $\epsilon = 4.8$ cm, $l = 35.2$ cm, ($\epsilon/l = 0.14$), $b = 1.6$ cm, $d_o = 0.05$ cm, $d_l = 0$.

The model, approaching actual conditions in its taper, was measured at $\alpha = 0^\circ$ and 10° . The results and the frequency curve by (2) are given in Figure 10. The blade exhibited violent torsional vibrations at the 10° setting, without however evincing any perceptible effect on the flexural vibrations.

Model 4.- Truncated pyramid, cut-off blade 3, same taper, but not to 0. Dimensions: $\epsilon = 4.8$ cm, $l = 27.7$ cm, ($\epsilon/l = 0.17$), $b = 1.6$ cm, $d_o = 0.05$ cm, $d_l = 0.01$ cm.

The data are likewise appended in Figure 10 and compared with the theoretical results.

Model 5.- Blade-twisted and curved. Dimensions: $\epsilon = 4.8$ cm, $l = 21.1$ cm, ($\epsilon/l = 0.23$), $b = 1.6$ cm, $d = 0.03$ cm.

After the preceding tests had demonstrated that equation (2) presented a sufficiently close approximation for blades of constant section and different taper, the succeeding models were selected for constant section because the influence of the camber and twist must necessarily become the more noticeable as the mass of the blade tip is greater.

The model blade was evenly twisted through 25° from root to tip. In addition, its axis was curved perpendicular to the direction of the tip section (i.e., thrust direction), that is, in a plane, sloping against the direction of restraint of the blade root, so that the blade was constrained to coupled vibrations in all degrees of freedom. The deflection at the tip amounted to 1 cm, i.e., $1/20$ of the blade length. To this is added the deflection due to air load. As a result the actual blade conditions were much exaggerated.

The blade was so restrained as to make the setting at the free end 0° and 12° . The measured flexural frequencies are shown in Figure 11. The close agreement between calculation and measurement manifests that the other degrees of freedom (because of their frequencies totally different from flexural frequency) leave the flexural vibrations practically unaffected.

Model 6.— Blade-twisted, cambered and crescent-shaped. (Fig. 12, scale 1:5.) Dimensions: $\epsilon = 4.9$ cm, $l = 20.3$ cm, ($\epsilon/l = 0.24$), $b = 1.8$ cm, $d = 0.03$ cm. The tip is raked to $1/5$ of the blade length; so that in conjunction with the thrust loading the blade had a spatially curved bar axis. The blade had furthermore a 6° twist. The model was again whirled at two settings of the end section. The results are shown in Figure 13. In this case also there is scarcely any tangible influence on the flexural frequencies. (Compare Figure 15 to Model 7.)

Model 7.— Blade-twisted, curved and crescent-shaped, contour and dimensions as for Model 6.

It differs from Model 6 by the 25° twist and thus assumes, even in unloaded attitude, a 2.73 cm, (i.e. $1/7$ of the blade length) deflection perpendicular to the plane of rotation. The spatial curvature of the bar axis exceeds by far the scale ever used in propellers. The setting of the root section was 33° , that of the tip section, 8° . At the measured speeds of $n = 0$ to 350 min. $^{-1}$, the elastic and the centrifugal forces are in the mutual relationship of normal propellers. A section for $n = 196$ min. $^{-1}$, and the corresponding evaluation is reproduced in Figures 14 and 15. It is seen that the flexure is superposed by a more rapid motion. That might be torsional vibration, for it is to be noted that a torsion of the root sections at the free

end of the curved blade is very similarly noticeable like a flexural motion, that is, essentially as parallel displacement of the outer sections. Only the frequency of this motion is a much higher one than that of the flexural vibration. In any case, a glance at Figure 15 readily shows that the frequency of the recorded flexural vibration can scarcely differ from the purely flexural vibration as would occur by stiffness of the torsion and as postulated in the calculation.

The frequencies measured at the different speeds are compiled in Figure 13. (Owing to the strong twist with respect to Model 6, the λ_0 value has grown to 314 min.⁻¹.) There is a slightly perceptible drop in the measured figures compared to the theoretical curve obtained from (2). But the discrepancy does not exceed 4 per cent, and so remains, even in this extreme case, appreciably less than the highest possible error of about 7 per cent.

V. SUMMARY

The previously (reference 6) developed formula for calculating the flexural frequencies of rotating propellers

$$\frac{\lambda}{\lambda_0} = \left[1 + \frac{7 \left(\frac{n}{\lambda_0} \right)^2}{6 + 7 \left(\frac{n}{\lambda_0} \right)} \right] \sqrt{\frac{1 + (1 + 2 \frac{e}{l}) \left(\frac{n}{\lambda_0} \right)^2}{1 + \left(\frac{n}{\lambda_0} \right)^2}}$$

can be applied to any existing blade form. A mathematical estimation of the error involved reveals that the greatest possible discrepancy does not exceed 7 per cent of the true value, even for spatially curved and twisted blades.

Model tests reveal the actual error to be considerably less than the maximum theoretical error. Even in extreme cases, in which the curvatures of real propellers has been many-fold exaggerated, the discrepancy between calculation and experiment did not exceed 4 per cent.

The evolved formula is therefore to be used as basis for the study of flexural vibrations. It stipulates the knowledge of frequency λ_0 of the non-rotating propeller. The quickest and safest way to define this value is by actual test rather than by calculation.

A low limit for the flexural frequencies is given by

$$\frac{\lambda}{\lambda_0} = \sqrt{1 + (1 + 2 \frac{c}{l}) (\frac{n}{\lambda_0})^2}$$

This term can be used for a first estimation.

Translation by J. Vanier,
National Advisory Committee
for Aeronautics.

REFERENCES

1. Stodola: Dampf und Gasturbinen, Section 195.
2. Hütte: I, 25. Auflage, p. 407.
3. Southwell, R. V. and Gough, Barbara S: The Free Transverse Vibrations of Airscrew Blades. R. & M. No. 766, British A.R.C., 1921.
4. Sörensen: Berechnung der Eigenschwingungszahlen von Dampf-turbinenschaukeln, Werft-Reederei-Hafen, 1928, p. 67.
5. Liebers, Fritz: Contribution to the Theory of Propeller Vibrations. T.M. No. 568, N.A.C.A., 1930.
6. Liebers, Fritz: Resonance Vibrations of Aircraft Propellers. T.M. No. 657, N.A.C.A., 1932.
7. Seewald, Friedrich: Flutter in Propeller Blades. T.M. No. 642, N.A.C.A., 1931.
8. Hoff, W: Research Work of the D.V.L., Journal, R.A.S., Vol. 35, No. 249, p. 771, 1931.
9. Hohenemser: Beitrag zur Dynamik des elastischen Stabes mit Anwendung auf den Propeller, Z.F.M., Vol. 23, No. 2, p. 37. 1932.

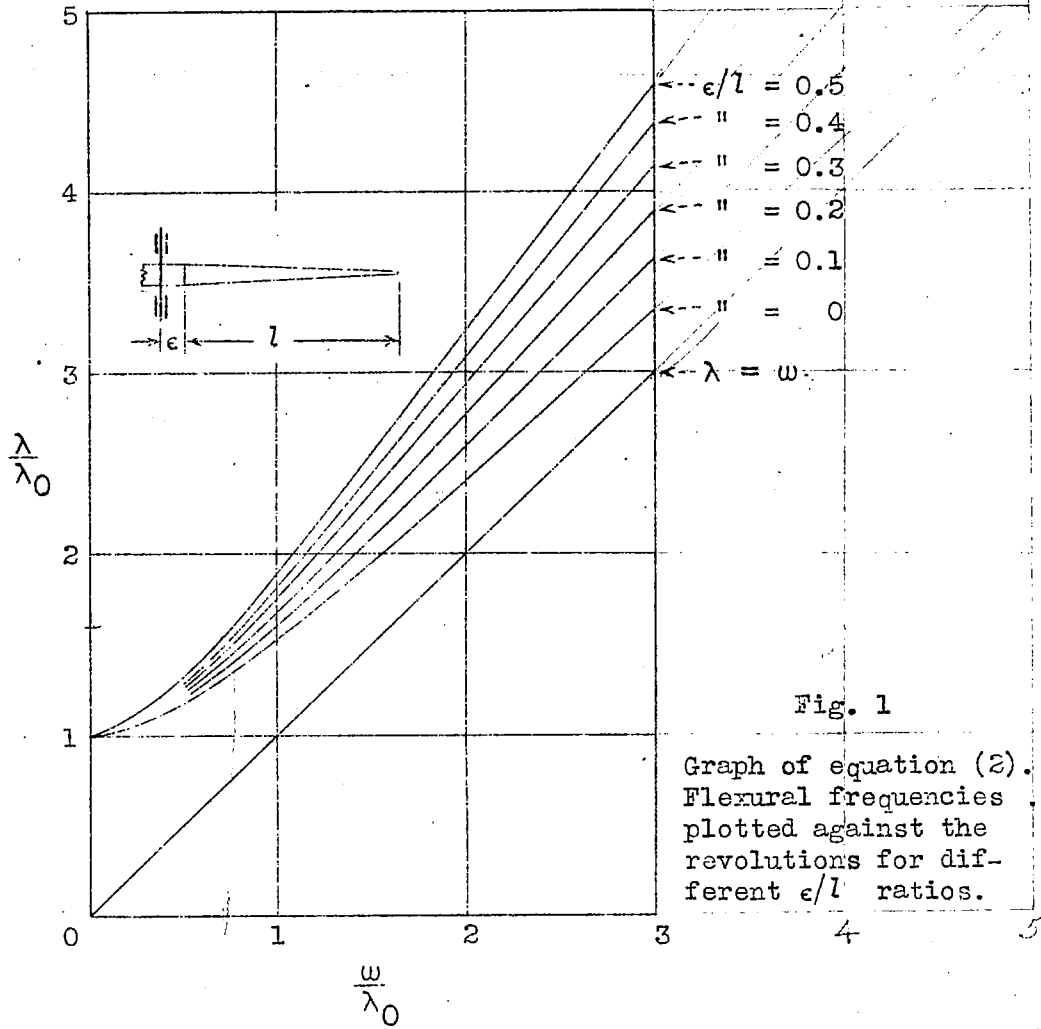


Fig. 1

Graph of equation (2). Flexural frequencies plotted against the revolutions for different ϵ/l ratios.

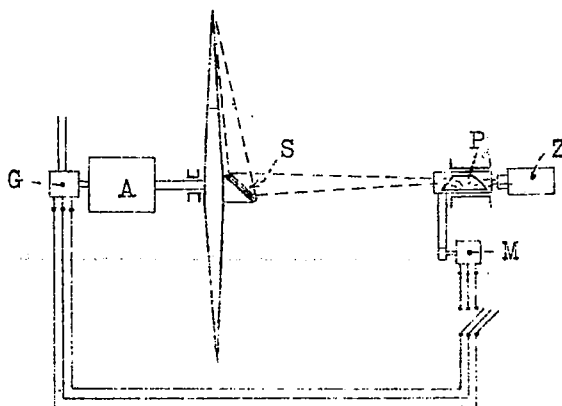


Fig. 2

Scheme of the arrangement for the observation of propeller vibrations.

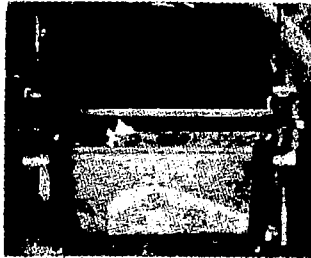
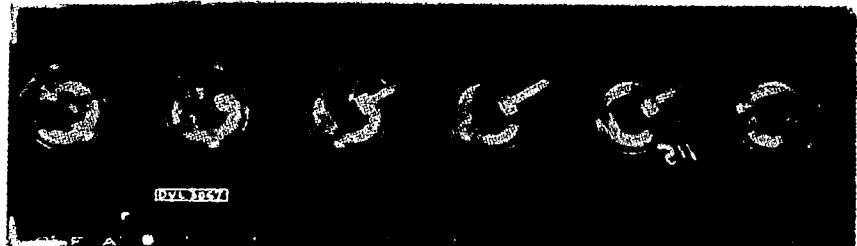


Fig.3 Picture of rotating propeller as seen by observer looking through the rotoscope. (The picture shows a full-size propeller. The arrangement of the mirror is somewhat different from that used in the model experiments. The plane of the mirror is adjustable).



CONTINUED BELOW



Fig.4 Part of film from test: model 1, $n = 496 \text{ min}^{-1}$ (128 pictures per second). The moving bright strip in the mirror is the blade tip, the white dot is the time mark.



CONTINUED BELOW



Fig.14 Part of film test: model 7 (twisted, spatially curved blade) $n = 196 \text{ min}^{-1}$. The strikingly bright strip is a mirror edge, used as reference axis.

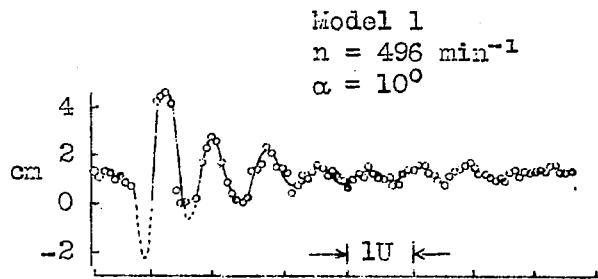


Fig.5 Elaboration of film of Fig.4. The vibration is slightly damped ($\alpha = 10^\circ$, $\frac{\partial c_a}{\partial \alpha} \approx 0$). The double arrow on the time scale marks the duration of one turn.

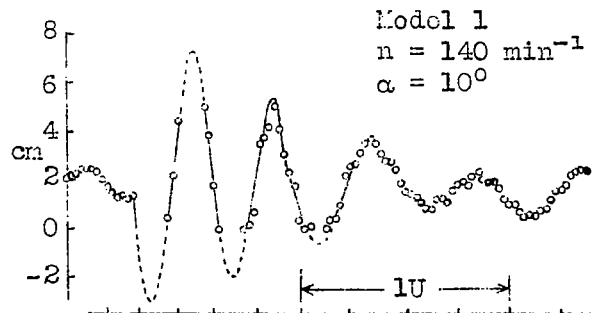


Fig.6 Vibration of model 1, at $n = 140 \text{ min}^{-1}$, $\alpha = 10^\circ$; slight damping ($\frac{\partial c_a}{\partial \alpha} \approx 0$).

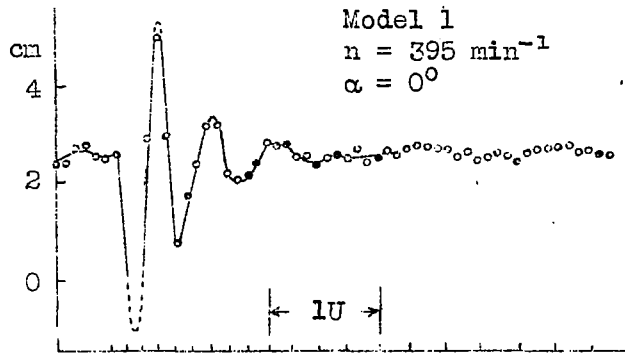


Fig.7 Vibration of model 1 at $n = 395 \text{ min}^{-1}$, $\alpha = 0^\circ$;
 considerable damping ($\frac{\partial c_a}{\partial \alpha} > 0$)

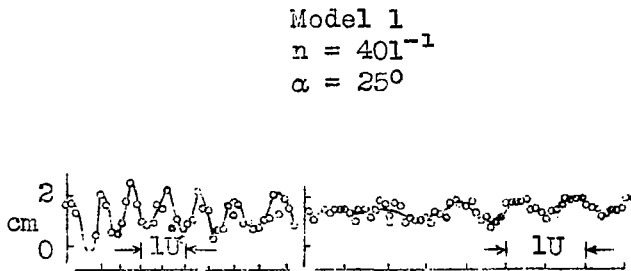


Fig.8 Vibration of model 1 at $n = 401 \text{ min}^{-1}$, $\alpha = 25^\circ$;
 steady or forced vibration ($\frac{\partial c_a}{\partial \alpha} < 0$).

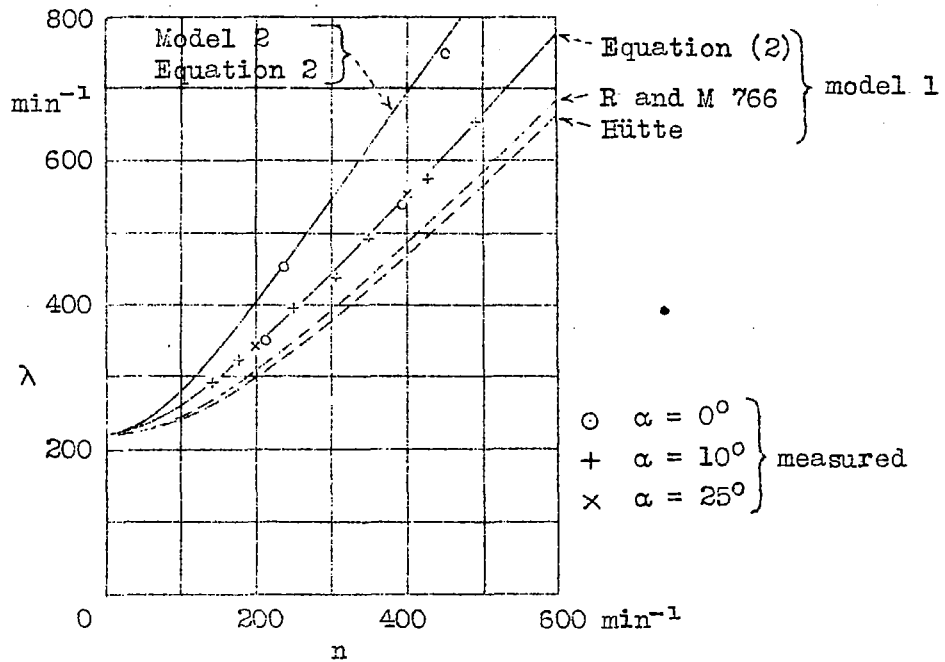


Fig. 9 Measured flexural frequencies of models 1 and 2 plotted against speed of rotation. Comparison between measurement and different calculations.

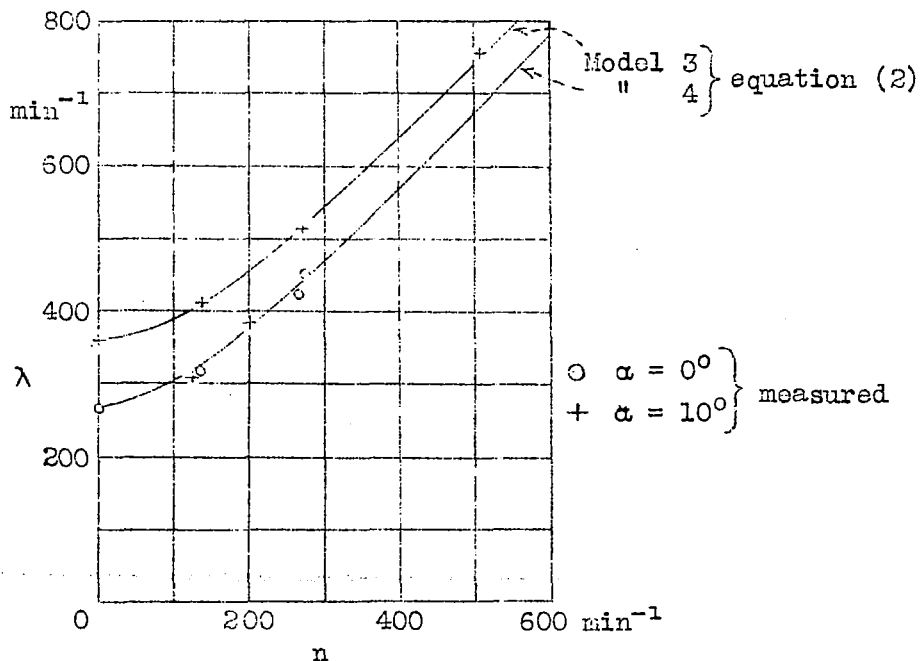


Fig. 10 Measured flexural frequencies of models 3 and 4 (straight, tapered blades). Calculation according to equation (2) compared with measurement.

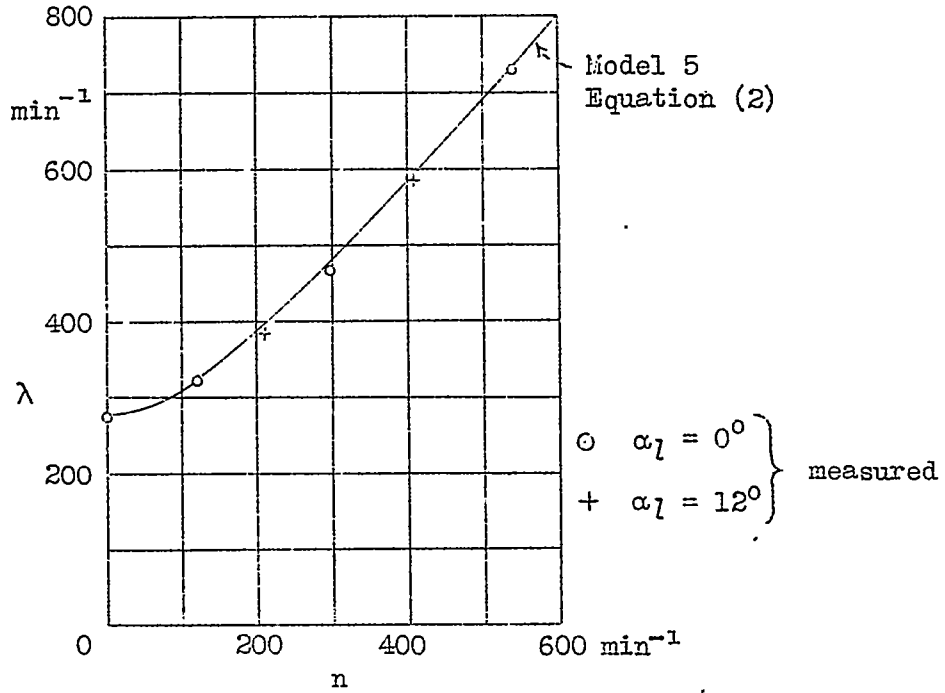


Fig. 11 Measured flexural frequencies of model 5 (twisted, curved blade). Comparison between measurement and calculation conformably to (2).

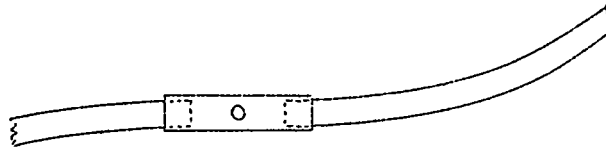


Fig. 12 Models 6 and 7. Projection on plane of propeller disk. Scale 1 : 5 ,

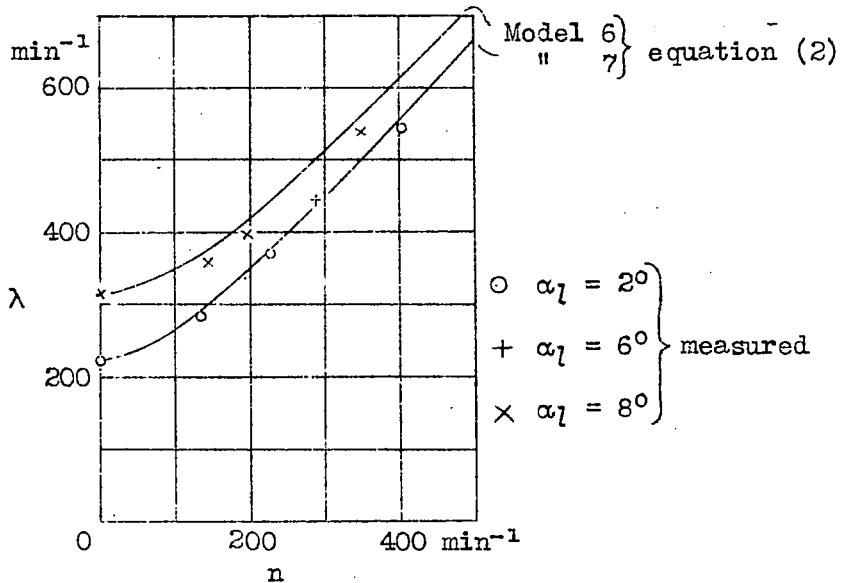


Fig. 13 Measured flexural frequencies of models 6 and 7; measurement compared to calculation according to (2).

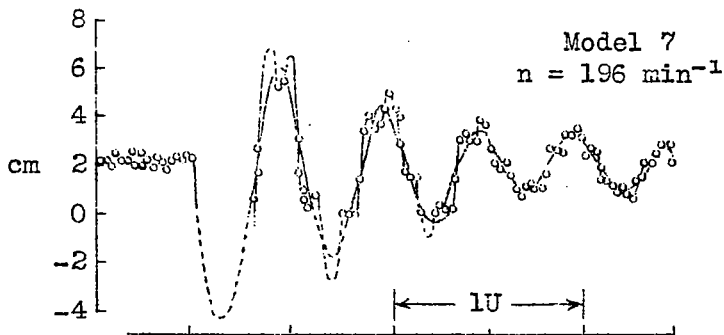


Fig. 15 Vibrations of model 7 at $n = 196 \text{ min}^{-1}$, Faster torsional vibrations are superimposed on the slow flexure.

NASA Technical Library



3 1176 01437 3527